Semiclassical perturbation Stark widths of singly charged argon spectral lines

Rafik Hamdi, Nabil Ben Nessib, Sylvie Sahal-Bréchot, Milan Dimitrijević

Monthly Notices
of the
ROYAL ASTRONOMICAL SOCIETY

MNRAS **475,** 800–813 (2018) doi:10.1093/mnras/stx3209

Semiclassical perturbation Stark widths of singly charged argon spectral lines

Rafik Hamdi,[1,2]★ Nabil Ben Nessib,[3] Sylvie Sahal-Bréchot[4] and Milan S. Dimitrijević[4,5,6,7]

[1]*Deanship of the Preparatory Year, Department of Physics, Umm Al-Qura University, Makkah, Kingdom of Saudi Arabia*
[2]*Groupe de Recherche en Physique Atomique et Astrophysique, Faculté des Sciences de Bizerte, Université de Carthage, Tunisia*
[3]*Department of Physics and Astronomy, College of Science, King Saud University. PO Box 2455, Riyadh 11451, Saudi Arabia*
[4]*LERMA, Observatoire de Paris, PSL Research University, CNRS, Sorbonne Universités, UPMC Univ., Paris 06, 5 Place Jules Janssen, F-92195 Meudon Cedex, France*
[5]*Astronomical Observatory, Volgina 7, 11060 Belgrade, Serbia*
[6]*IHIS-Techno Experts, Bezanijski put 23, 11080 Belgrade-Zemun, Serbia*
[7]*Institute Isaac Newton of Chile, Yugoslavia Branch, 11060 Belgrade, Serbia*

Accepted 2017 December 6. Received 2017 November 11; in original form 2017 October 25

ABSTRACT

Using a semiclassical perturbation approach with the impact approximation, Stark widths for singly charged argon (Ar II) spectral lines have been calculated. Energy levels and oscillator strengths needed for this calculation have been determined using the Hartree–Fock method with relativistic corrections. Our Stark widths are compared with experimental results for 178 spectral lines. Our results may be of interest not only for laboratory plasma, lasers and technological plasmas but also for white dwarfs and A- and B-type stars.

Key words: atomic data – atomic processes – line: formation.

1 INTRODUCTION

Stark broadening is an important broadening mechanism in both laboratory and astrophysical plasmas. Stark broadening parameters (width and shift) are needed in opacity calculations, stellar atmosphere modelling and the determination of the abundance of chemical elements. Stark broadening is one of the methods used in plasma characterization. For example, this method is used by Qian et al. (2010) in the determination of electron density in an atmospheric argon plasma. Dimitrijević & Csillag (2006) used Stark broadening of the Ar II 476.5 nm spectral line to explain the single-mode operation of the He–Ar II 476.5 nm laser.

The influence of Stark broadening in stellar atmospheres of A-type and B-type stars is studied in several papers (Popović et al. 2001; Simić et al. 2005, 2009). Based on the atmosphere models in Wesemael (1981), Hamdi et al. (2008) and Dimitrijević et al. (2015) studied the influence of Stark broadening in DO white dwarf atmospheres for the spectral lines of Si VI and Xe VIII, respectively. It was found that Stark broadening is dominant in comparison with thermal Doppler broadening, especially for atmospheres with a high surface gravity. In Hamdi et al. (2014, 2017), the importance of Stark broadening is investigated for subdwarf B stars using Ar II and Ar III spectral lines. This study is based on plane-parallel line-blanketed model atmospheres (Jeffery, Woolf & Pollacco 2001).

A number of Ar II spectral lines were observed by Lanz et al. (2008) in the optical spectra of early B-type stars. In Lanz et al. (2008), 11 Ar II spectral lines were analysed and argon abundance was determined from best fits between the observed and synthetic spectra. Besides B-type stars, Ar II spectral lines are also used in the determination of argon abundance in subdwarf B stars (Heber & Edelmann 2004; Blanchette et al. 2008; Naslim et al. 2012).

Djurović et al. (2013) reported 126 experimental Stark widths for Ar II spectral lines in the spectral range from 265 to 405 nm. For a number of transitions given in Djurović et al. (2013), there is no other experimental or theoretical results for comparison. Pellerin, Musiol & Chapelle (1997) and Aparicio et al. (1998) also give a large number of widths. For some transitions, there is a large difference between the different experimental results. Dimitrijević & Truong-Bach (1986) carried out semiclassical perturbation (SCP) calculations of the Stark broadening parameters of Ar II spectral lines. The energy levels were taken from Bashkin & Stoner (1975) and oscillator strengths were calculated using a scaled Thomas–Fermi model (Stewart & Rotenberg 1965). Dimitrijević & Csillag (2006) performed SCP calculations of the Stark width for two multiplets (476.5 and 480.6 nm) using energy levels from Bashkin & Stoner (1975) and oscillator strengths calculated using the Bates & Damgaard method. A sophisticated SCP calculation of Stark broadening parameters for a large number of spectral lines of Ar II would be useful in improving the investigation of this broadening mechanism. Such calculations are also of interest for checking theory and experiments.

★ E-mail: Rafik.Hamdi@istls.rnu.tn

In this paper, we have determined Stark widths for 300 spectral lines of Ar II. The impact SCP approach (Sahal-Bréchot 1969a,b) and a set of atomic data calculated using the Hartree–Fock method with relativistic corrections (HFR) (Cowan 1981) have been used. Results are given for collisions with electrons, protons, and singly charged helium and singly charged argon ions. In this work, we are interested in transitions of the type: 3d–4p, 4s–4p, 4p–4d and 4p–5s. To check the accuracy of our results, we compared our Stark widths with experimental results for 178 spectral lines. We have also investigated the temperature dependence of the Stark widths. In Hamdi et al. (2017), we have compared our Stark widths with the experimental results for 34 transitions belonging to the 3d–4p transition array. In previous works (Hamdi et al. 2011, 2013, 2014), the same method was used and we determined Stark broadening parameters for 114 spectral lines of Pb IV and 14 spectral lines of Ar III.

The present paper is organized as follow. In Section 2, an outline of the impact SCP theory is given. In Section 3, we compare our results with experimental and other theoretical results. In Section 4, our Stark widths are compared with previous SCP calculations and in Section 5, our large-scale calculations are presented.

2 THE IMPACT SEMICLASSICAL PERTURBATION METHOD

A detailed description of this formalism with all the innovations is given in Sahal-Bréchot (1969a,b, 1974, 1991), Fleurier, Sahal-Bréchot & Chapelle (1977), Dimitrijević, Sahal-Bréchot & Bommier (1991), Dimitrijević & Sahal-Bréchot (1996) and Sahal-Bréchot, Dimitrijević & Ben Nessib (2014). The profile $F(\omega)$ is Lorentzian for isolated lines:

$$F(\omega) = \frac{w/\pi}{(\omega - \omega_{if} - d)^2 + w^2} \tag{1}$$

where d is the shift and

$$\omega_{if} = \frac{E_i - E_f}{\hbar}.$$

i and f denote the initial and final states and E_i and E_f their corresponding energies.

The total width at half-maximum ($W = 2w$) (in angular frequency units) of an electron-impact broadened spectral line can be expressed as

$$W = N \int v f(v)\, \mathrm{d}v \left(\sum_{i' \neq i} \sigma_{ii'}(v) + \sum_{f' \neq f} \sigma_{ff'}(v) + \sigma_{\mathrm{el}} \right), \tag{2}$$

where N is the electron density, $f(\upsilon)$ is the Maxwellian velocity distribution function for electrons and ρ is the impact parameter of the incoming electron. i' (respectively, f') denotes the perturbing levels of the initial state i (respectively, final state f). The inelastic cross-section $\sigma_{ii'}(\upsilon)$ (respectively, $\sigma_{ff'}(\upsilon)$) can be expressed by an integral over the impact parameter ρ of the transition probability $P_{ii'}(\rho, \upsilon)$ (respectively, $P_{ff'}(\rho, \upsilon)$) as

$$\sum_{i' \neq i} \sigma_{ii'}(\upsilon) = \frac{1}{2}\pi R_1^2 + \int_{R_1}^{R_\mathrm{D}} 2\pi\rho\, \mathrm{d}\rho \sum_{i' \neq i} P_{ii'}(\rho, \upsilon). \tag{3}$$

The elastic cross-section is given by

$$\sigma_{\mathrm{el}} = 2\pi R_2^2 + \int_{R_2}^{R_\mathrm{D}} 2\pi\rho\, \mathrm{d}\rho \sin^2\delta + \sigma_r,$$

$$\delta = \left(\varphi_\mathrm{p}^2 + \varphi_\mathrm{q}^2\right)^{\frac{1}{2}}. \tag{4}$$

The phase shifts φ_p and φ_q due, respectively, to the polarization potential (r^{-4}) and to the quadrupolar potential (r^{-3}), are given in section 3 of chapter 2 in Sahal-Bréchot (1969a). R_D is the Debye radius. All the cut-offs R_1, R_2 and R_3 are described in section 1 of chapter 3 in Sahal-Bréchot (1969b). σ_r is the contribution of the Feshbach resonance (Fleurier et al. 1977).

The formulae for the ion-impact widths are analogous to equations (2) and (3), without the Feshbach resonance contribution to the width. For electrons, hyperbolic paths due to the attractive Coulomb force are used, while for perturbing ions, the hyperbolic paths are different since the force is repulsive.

The main input parameters used in the SCP calculation of Stark broadening parameters are energy levels and oscillator strengths. The set of atomic data needed for the semiclassical method is relatively large. When the set of atomic data for an atom or ion is not complete, the SCP method cannot be applied in an adequate way. In this case, one can use a modified semi-empirical formula (Dimitrijević & Konjević 1980) since this method needs less atomic data.

In our present calculations, energy levels and oscillator strengths are from the HFR approach using the Cowan code (Cowan 1981). We use an atomic model including 24 configurations: $3s^2\ 3p^5$; $3s^2\ 3p^4\ nl$ (nl = 4p, 4f, 5p, 5f, 6p, 6f, 6h, 7p, 7f and 7h) (odd parity) and $3s\ 3p^6$; $3s^2\ 3p^4\ n'l'$ ($n'l'$ = 3d, 4s, 4d, 5s, 5d, 5g, 6s, 6d, 6g, 7s, 7d and 7g) (even parity). We use an ab initio procedure.

To introduce a correction to the widths due to the difference between calculated and experimental wavelengths, we have used equation (8) of Hamdi et al. (2013).

3 STARK WIDTHS

In Table 1, we compare our Stark widths with the experimental results of Djeniže et al. (1989), Dzierzega & Musiol (1994), Pellerin et al. (1997), Aparicio et al. (1998), Iglesias et al. (2006), Djurović et al. (2013) and Gajo et al. (2013). In this way, our results are compared with all the experimental results published since 1989. In Table 1, our Stark widths are compared also with results in Griem (1974).

The plasma source used in the different experiments was a low-pressure pulsed arc in Aparicio et al. (1998), Djurović et al. (2013) and Djeniže et al. (1989); a wall stabilized arc in Dzierzega & Musiol (1994), Pellerin et al. (1997) and Gajo et al. (2013); and a laser plasma in Iglesias et al. (2006). For the electron temperature measurements, the Boltzmann plot technique was used by Dzierzega & Musiol (1994), Aparicio et al. (1998), Djurović et al. (2013) and Gajo et al. (2013). Pellerin et al. (1997) used the Larenz–Fowler–Milne method, a Olsen–Richter graph and the relative intensities of two Ar II lines. Djeniže et al. (1989) used a Boltzmann plot of Ar II lines and the ratio of Ar III to Ar II lines. In Iglesias et al. (2006), besides the ratio of He II to He I line intensities, the Stark broadening of He II and He I were also used. To measure the electron density, laser interferometry at 6328 Å was used by Aparicio et al. (1998), Djurović et al. (2013) and Djeniže et al. (1989). Dzierzega & Musiol (1994) used the H β Stark width and continuum intensity. Pellerin et al. (1997) used plasma composition data and the Stark width of the Ar I 6965.43 Å line. In Iglesias et al. (2006), the Stark widths of He I and He II spectral lines were used. Gajo et al. (2013) used the Stark width of the H β spectral line. In Aparicio et al. (1998), Stark widths are given for a normalized electron density but not for a specified temperature. In Iglesias et al. (2006), Stark widths are measured for a high temperature (T = 43 000 K) compared to the other experiments and for three values of electron density.

Table 1. Our electron-impact Stark widths (FWHM) (W_e) and ion impact Stark width (W_i) calculated using the SCP approach with the impact approximation (Sahal-Bréchot 1969a,b) compared with experimental Stark widths (W_m) and the Stark width of Griem (1974), W_G. Transitions, wavelengths, electron temperature (T) and electron density (N_e) are also given. Ref.: a: Djeniže et al. (1989), b: Dzierzega & Musiol (1994), c: Pellerin et al. (1997), d: Aparicio et al. (1998), e: Iglesias et al. (2006), f: Djurović et al. (2013) and g: Gajo et al. (2013). All wavelengths are taken from the NIST data base (Kramida et al. 2015).

Transition array	Transition	λ (Å)	T (10^3 K)	N_e (10^{17} cm^{-3})	W_m (pm)	W_e (pm)	W_i (pm)	W_m/W	W_G (pm)	Acc.	Ref.
(^{3}P) 3d–(^{1}D) 4p	$^2F_{5/2}$–$^2F^o_{7/2}$	4904.75	22.0	1.00	36.9	47.0	9.14	0.66		B	c
			18.4–26.5	1.00	38.9	49.9–44.3	8.93–9.31	0.65–0.73		B+	d
	$^2F_{7/2}$–$^2F^o_{7/2}$	4682.28	22.0	1.00	29.2	43.8	8.25	0.56		C+	c
	$^2F_{7/2}$–$^2F^o_{5/2}$	4710.82	22.0	1.00	31.9	44.4	8.42	0.60		B	c
	$^2F_{5/2}$–$^2D^o_{5/2}$	4300.65	22.0	1.00	39.2	37.4	7.9	0.87		B	c
			18.4–25.6	1.00	46.4	39.8–35.1	7.72–8.01	0.98–1.08		B+	d
	$^2D_{5/2}$–$^2F^o_{7/2}$	5141.78	18.4–26.5	1.00	33.2	55.3–49.3	9.88–10.3	0.51–0.56		B+	d
	$^2D_{3/2}$–$^2F^o_{5/2}$	5017.16	18.4–26.5	1.00	43.7	54.2–48.1	9.35–9.79	0.69–0.75		B	d
	$^2D_{5/2}$–$^2F^o_{5/2}$	5176.23	18.4–26.5	1.00	44.8	55.9–49.9	9.99–10.4	0.68–0.74		B+	d
	$^2D_{5/2}$–$^2D^o_{5/2}$	4481.81	10.88	2.03	78.0	108	–	0.72		B+	b
			11.52	1.79	47.7	93.5	–	0.51		B+	b
			13.03	1.10	33.0	54.6	8.65	0.52		A	b
			13.88	1.39	42.8	67.3	11.0	0.55		B+	b
			22.0	1.00	37.3	40.9	8.56	0.75		B	c
	$^2D_{3/2}$–$^2D^o_{5/2}$	4362.07	18.4–26.5	1.00	33.3	42.6–37.6	7.93–8.22	0.66–0.73		B+	d
	$^2D_{5/2}$–$^2D^o_{3/2}$	4490.98	22.0	1.00	39.5	45.6	8.69	0.73		B	c
			18.4–26.5	1.00	38.2	48.4–43.0	8.50–8.84	0.67–0.74		B+	d
	$^2P_{3/2}$–$^2P^o_{3/2}$	3766.12	18.4–26.5	1.00	101.4	38.8–34.4	6.14–6.45	2.25–2.48		B+	d
	$^2P_{1/2}$–$^2P^o_{3/2}$	3634.81	22.0	1.00	49.09	34.12	5.94	1.22		C	f
	$^2P_{3/2}$–$^2D^o_{5/2}$	3605.88	22.0	1.00	25.50	24.1	5.49	0.86		C	f
	$^2D_{3/2}$–$^2P^o_{1/2}$	4474.76	22.0	1.00	109.7	64.6	9.43	1.48		B	c
			18.4–26.5	1.00	128.6	68.0–61.1	9.10–9.62	1.67–1.82		B+	d
	$^2D_{3/2}$–$^2P^o_{3/2}$	4598.76	18.4–26.5	1.00	83.8	63.8–56.5	9.16–9.68	1.15–1.27		B+	d
	$^2F_{5/2}$–$^2P^o_{3/2}$	4530.55	18.4–26.5	1.00	76.8	61.0–54.1	8.90–9.42	1.10–1.21		B+	d
(^{3}P) 4s–(^{3}P) 4p	$^4P_{5/2}$–$^4P^o_{5/2}$	4806.02	10.88	2.03	48.4	104.9	7.62	0.43	83.4	B+	b
			11.52	1.79	44.0	90.3	6.85	0.45	71.0	B+	b
			12.2	0.74	15.7	36.6	2.91	0.40	29.1	A	b
			13.03	1.10	23.2	52.9	4.37	0.41	42.2	A	b
			13.88	1.39	30.5	65.2	5.57	0.43	52.6	B+	b
			22.0	1.00	32.3	39.5	4.37	0.74	34.4	B	c
			17.0–26.7	1.00	28.8	43.9–37.3	4.18–4.51	0.60–0.69	35.6–33.9	B+	d
			13.4	1.3	40.0	61.8	5.18	0.59	51.1	B+	g
			14.2	1.6	50.0	74.3	6.42	0.62	61.9	B+	g
	$^4P_{3/2}$–$^4P^o_{3/2}$	4933.21	22.0	1.00	32.2	42.9	4.71	0.68	36.6	B	c
			18.1–24.4	1.00	32.5	46.9–41.3	4.57–4.88	0.63–0.70	37.4–36.1	B+	d
			13.4	1.30	50.0	68.8	5.6	0.67	53.3	B+	g
			14.2	1.60	55.0	82.7	6.94	0.61	64.5	B+	g
	$^4P_{1/2}$–$^4P^o_{1/2}$	4972.16	22.0	1.00	34.9	43.8	4.79	0.72	37.1	B	c
			16.5–23.2	1.00	29.5	48.9–42.7	4.55–4.84	0.55–0.62	38.3–36.9	B+	d
	$^4P_{5/2}$–$^4P^o_{3/2}$	4735.90	13.4	1.30	39	61.4	4.18	0.59	49.3	B+	g
			14.2	1.60	50	73.7	5.27	0.63	59.7	B+	g
	$^4P_{3/2}$–$^4P^o_{1/2}$	4847.81	10.88	2.03	54.5	111	7.98	0.46	83.8	B+	b
			11.52	1.79	46.1	95.5	7.18	0.45	72.0	B+	b
			12.20	0.74	22.2	38.7	3.05	0.53	29.2	A	b
			13.03	1.10	30.3	56.0	4.57	0.50	42.7	A	b
			13.88	1.39	36.6	68.9	5.83	0.49	52.3	B +	b
			22.0	1.00	33.8	41.3	4.57	0.74	35.2	B	c
			17.0–26.7	1.00	29.6	45.8–38.9	4.38–4.72	0.59–0.68	36.1–34.4	B+	d
			43.0	4.50	110	157	22.4	0.61	137	B	e
			43.0	7.20	170	252	35.7	0.59	220	B	e
			43.0	9.00	290	315	44.5	0.80	274	B	e
			13.4	1.3	45.0	65.4	5.41	0.64	51.5	B+	g
			14.2	1.6	56.0	68.8	5.89	0.75	62.5	B+	g
	$^4P_{3/2}$–$^4P^o_{5/2}$	5009.33	22.0	1.00	34.5	43.9	4.77	0.71	37.5	B	c
			16.5–23.2	1.00	28.7	49.4–43.0	4.52–4.81	0.53–0.60	42.2–37.3	B+	d
			13.4	1.30	54.0	69.9	5.65	0.71	55.2	B+	g
			14.2	1.60	61.0	83.9	7.00	0.67	66.9	B+	g

Table 1 – *continued*

Transition array	Transition	λ (Å)	T (10^3 K)	N_e (10^{17} cm^{-3})	W_m (pm)	W_e (pm)	W_i (pm)	W_m/W	W_G (pm)	Acc.	Ref.
	$^4P_{1/2}$–$^4P^o_{3/2}$	5062.04	22.0	1.00	40.3	45.5	4.96	0.80	38.4	B	c
			16.5–23.2	1.00	32.4	51.3–44.6	4.70–5.00	0.58–0.65	40.0–38.1	B+	d
			13.4	1.30	55.0	72.8	5.82	0.70	56.4	B+	g
			14.2	1.60	63.0	87.3	7.28	0.67	68.4	B+	g
	$^4P_{5/2}$–$^4D^o_{7/2}$	4348.06	22.0	1.00	29.2	33.6	3.84	0.78	28.9	B	c
			20.9–31.8	1.00	23.9	34.3–30.4	3.80–4.05	0.63–0.70	29.1–27.2	B+	d
			43.0	4.50	190	129	18.7	1.29	111	B	e
			43.0	7.20	260	206	29.8	1.10	177	B	e
			43.0	9.00	350	259	37.2	1.18	222	B	e
	$^4P_{3/2}$–$^4D^o_{5/2}$	4426.00	10.88	2.03	54.6	97.0	7.08	0.52	73.8	B+	b
			11.52	1.79	47.5	83.9	6.37	0.53	61.7	B+	b
			12.20	0.74	19.3	33.9	2.71	0.53	25.1	A	b
			13.03	1.10	29.4	49.1	4.04	0.55	36.3	A	b
			13.88	1.39	34.0	60.4	5.15	0.52	44.7	B+	b
			22.0	1.00	30.5	36.2	4.06	0.76	29.9	B	c
	$^4P_{1/2}$–$^4D^o_{3/2}$	4430.19	22.0	1.00	28.4	36.0	4.11	0.71	29.6	B	c
	$^4P_{5/2}$–$^4D^o_{5/2}$	4266.53	22.0	1.00	32.0	32.9	3.76	0.87	27.8	B	c
			18.4–26.5	1.00	25.2	35.2–31.2	3.66–3.89	0.65–0.72	28.3–27.1	B+	d
	$^4P_{3/2}$–$^4D^o_{3/2}$	4331.20	22.0	1.00	33.8	34.2	3.94	0.87	28.6	B	c
			43.0	4.50	180	131	19.1	1.20	109	B	e
			43.0	7.20	220	209	30.5	0.92	175	B	e
			43.0	9.00	300	261	38.0	1.00	219	B	e
	$^4P_{1/2}$–$^4D^o_{1/2}$	4379.67	10.88	2.09	45.7	101	7.31	0.42	72.5	B+	b
			11.52	1.79	42.9	84.5	6.39	0.47	60.4	B+	b
			12.20	0.74	18.6	34.1	2.71	0.51	24.5	A	b
			13.03	1.10	28.4	49.3	4.06	0.53	35.5	A	b
			13.88	1.39	42.9	60.6	5.17	0.65	43.8	B+	b
			22.0	1.00	31.6	36.0	4.05	0.79	29.5	B+	c
	$^4P_{5/2}$–$^4D^o_{3/2}$	4178.36	22.0	1.00	32.0	31.1	3.66	0.92	26.7	B	c
	$^4P_{3/2}$–$^4D^o_{1/2}$	4282.90	22.0	1.00	25.2	34.1	3.89	0.66	28.0	B	c
			18.4–26.5	1.00	20.0	36.9–32.3	3.77–4.00	0.49–0.55	28.6–27.4	B+	d
	$^4P_{5/2}$–$^2D^o_{5/2}$	4082.39	18.4–26.5	1.00	33.8	34.7–30.8	3.50–3.70	0.88–0.98		B+	d
	$^4P_{3/2}$–$^2D^o_{3/2}$	4112.82	22.0	1.00	22.1	34.8	3.78	0.57		B	c
	$^4P_{3/2}$–$^2D^o_{5/2}$	4228.16	22.0	1.00	29.9	35.7	3.86	0.76		B	c
			18.4–26.5	1.00	33.1	38.4–33.9	3.75–3.98	0.79–0.87		C+	d
	$^4P_{5/2}$–$^2D^o_{3/2}$	3974.76	22.0	1.00	22.91	31.6	3.53	0.65		C	f
	$^4P_{5/2}$–$^2P^o_{3/2}$	3845.40	22.0	1.00	21.53	27.6	3.26	0.70		B	f
	$^4P_{3/2}$–$^2P^o_{3/2}$	3974.48	22.0	1.00	22.42	30.3	3.65	0.66		B	f
	$^4P_{5/2}$–$^4S^o_{3/2}$	3729.31	22.0	1.00	22.9	25.0	3.19	0.81		B	c
			22.0	1.00	16.62	25.0	3.19	0.59		C	f
			11.88	2.03	38.1	67.8	5.61	0.52		B+	b
			11.52	1.79	31.0	58.3	5.03	0.49		B+	b
			12.20	0.74	16.6	23.6	2.14	0.65		A	b
			13.03	1.10	19.0	34.0	3.19	0.51		A	b
			13.88	1.39	22.2	41.8	4.08	0.48		B+	b
	$^4P_{3/2}$–$^4S^o_{3/2}$	3850.58	10.88	2.03	48.6	74.2	5.96	0.61		B+	b
			11.52	1.79	32.8	63.7	5.34	0.48		B+	b
			12.20	0.74	18.6	25.7	2.27	0.66		A	b
			13.03	1.10	20.2	37.0	3.40	0.50		A	b
			13.88	1.39	26.8	45.5	4.33	0.54		A	b
			22.0	1.00	23.5	27.0	3.39	0.77		B	c
			18.4–26.5	1.00	25.7	29.1–25.3	3.29–3.48	0.79–0.89		A	d
			22.0	1.00	17.12	27.0	3.39	0.57		C	f
	$^4P_{1/2}$–$^4S^o_{3/2}$	3928.62	26.0	1.76	34.0	46.6	6.35	0.64		B	a
			10.88	2.03	50.4	77.5	6.19	0.60		B+	b
			11.52	1.79	31.8	66.6	5.55	0.44		B+	b
			12.20	0.74	18.0	26.9	2.36	0.62		A	b
			13.03	1.10	24.4	38.7	3.53	0.60		A	b
			22.0	1.00	23.3	28.2	3.52	0.73		B	c
			18.4–26.5	1.00	33.6	30.4–26.4	3.34–3.63	1.00–1.12		B+	d
			22.0	1.00	17.82	28.2	3.52	0.56		C	f

Table 1 – *continued*

Transition array	Transition	λ (Å)	T (10^3 K)	N_e (10^{17} cm^{-3})	W_m (pm)	W_e (pm)	W_i (pm)	W_m/W	W_G (pm)	Acc.	Ref.
	$^2P_{3/2}$–$^4D^o_{5/2}$	5145.31	22.0	1.00	41.5	48.4	5.39	0.77		B	c
			18.4–26.5	1.00	22.3	51.9–46.0	5.34–5.66	0.40–0.43		B+	d
	$^2P_{3/2}$–$^2D^o_{5/2}$	4879.86	10.88	2.03	72.8	124	10.78	0.54		B+	b
			11.52	1.79	58.7	108	8.07	0.51		B+	b
			12.20	0.74	23.4	43.4	3.42	0.50		B+	b
			13.03	1.10	37.0	62.8	5.13	0.54		A	b
			13.88	1.39	45.4	77.2	6.54	0.54		B+	b
			13.4	1.3	56.0	73.2	6.08	0.71		B+	g
			14.2	1.6	70.0	88.1	7.55	0.73		B+	g
	$^2P_{1/2}$–$^2D^o_{3/2}$	4965.08	10.88	2.03	76.4	134	9.56	0.53		B+	b
			11.52	1.79	58.7	116	8.59	0.47		B+	b
			12.2	0.74	28.5	46.6	3.68	0.57		A	b
			13.03	1.10	36.6	67.4	5.47	0.50		A	b
			13.88	1.39	47.2	82.9	6.98	0.53		B+	b
			16.5–23.2	1.00	39.0	55.7–48.8	5.22–5.52	0.64–0.72		B+	d
			13.4	1.3	60.0	78.8	6.48	0.70		B+	g
			14.2	1.6	71.0	94.6	8.04	0.69		B+	g
	$^2P_{3/2}$–$^2D^o_{3/2}$	4726.87	10.88	2.03	74.1	122	8.72	0.57		B+	b
			11.52	1.79	59.4	106	7.84	0.52		B+	b
			12.20	0.74	18.4	42.6	3.33	0.40		B+	b
			13.03	1.10	35.6	61.6	5.00	0.53		B+	b
			22.0	1.00	39.3	45.4	5.00	0.78		B	c
			13.4	1.3	55	72.0	5.91	0.70		B+	g
			14.2	1.6	63	86.5	7.34	0.67		B+	g
	$^2P_{3/2}$–$^2P^o_{3/2}$	4545.05	10.88	2.03	61.4	104	8.40	0.55		B+	b
			11.52	1.79	50.4	89.6	7.50	0.52		B+	b
			12.20	0.74	25.2	36.2	3.18	0.64		A	b
			13.03	1.10	32.0	52.3	4.77	0.56		A	b
			13.88	1.39	39.6	64.5	6.08	0.56		A	b
			22.0	1.00	36.2	38.8	4.77	0.83		B	c
	$^2P_{1/2}$–$^2P^o_{1/2}$	4889.04	22.0	1.00	38.6	45.0	5.54	0.76		B	c
	$^2P_{3/2}$–$^2P^o_{1/2}$	4657.90	10.88	2.03	58.7	109	8.76	0.50		B+	b
			11.52	1.79	46.4	94.0	7.87	0.46		B+	b
			12.20	0.74	23.6	37.9	3.34	0.57		A	b
			13.03	1.10	34.2	54.9	5.00	0.57		A	b
			13.88	1.39	40.4	67.6	6.38	0.55		B+	b
			22.0	1.00	37.0	40.7	5.00	0.81		B	c
			17.0–26.7	1.00	32.8	45.0–38.3	4.78–5.14	0.66–0.76		B+	d
			13.4	1.3	49	64.2	5.93	0.70		B+	g
			14.2	1.6	58	77	7.37	0.69		B+	g
	$^2P_{1/2}$–$^2P^o_{3/2}$	4764.86	10.88	2.03	75.0	114	9.19	0.61		B+	b
			11.52	1.79	49.6	98.4	8.26	0.47		B+	b
			12.20	0.74	22.6	39.7	3.50	0.52		A	b
			13.03	1.10	34.6	57.4	5.25	0.55		A	b
			13.88	1.39	42.6	70.7	6.70	0.55		B+	b
			22.0	1.00	38.4	42.7	5.21	0.80		B	c
			17.0–26.7	1.00	34.0	47.1–40.1	5.02–5.40	0.65–0.75		B+	d
			43.0	4.50	160	162	24.4	0.86		B	e
			43.0	7.20	200	260	40.5	0.67		B	e
			43.0	9.00	240	326	–	0.74		B	e
			13.4	1.30	58	66.6	6.23	0.80		B+	g
			14.2	1.60	64	80.6	7.73	0.72		B+	g
	$^2P_{3/2}$–$^4S^o_{3/2}$	4383.75	18.4–26.5	1.00	41.3	37.0–32.6	4.28 - 4.52	1.00–1.11		B+	d
	$^2P_{3/2}$–$^2S^o_{1/2}$	4375.95	22.0	1.00	24.4	36.8	4.46	0.59		C+	c
	$^2P_{1/2}$–$^2S^o_{1/2}$	4579.35	10.88	2.03	68.8	105	8.61	0.61		B+	b
			11.52	1.79	48.7	92.8	7.62	0.48		B+	b
			12.20	0.74	18.4	38.4	3.21	0.44		B+	b
			13.88	1.39	32.2	72.1	5.97	0.41		B+	b
			22.0	1.00	36.3	40.1	4.91	0.81		B	c
			16.5–23.2	1.00	32.2	44.3–39.5	4.77–5.04	0.66–0.72		B+	d
			13.40	1.30	47	62.1	5.82	0.69		B+	g
			14.20	1.60	53	74.8	7.23	0.65		B+	g

Table 1 – *continued*

Transition array	Transition	λ (Å)	T (10^3 K)	N_e (10^{17} cm^{-3})	W_m (pm)	W_e (pm)	W_i (pm)	W_m/W	W_G (pm)	Acc.	Ref.
(^{3}P) 4s–(^{1}D) 4p	$^2P_{3/2}$–$^2D^o_{5/2}$	2844.13	26.0	1.76	25.8	33.4	5.99	0.65		B	a
			22.0	1.00	16.73	20.1	3.34	0.71		C	f
	$^2P_{3/2}$–$^2D^o_{3/2}$	2847.82	22.0	1.00	13.8	19.8	3.28	0.60		C+	c
	$^2P_{1/2}$–$^2D^o_{3/2}$	2932.59	22.0	1.00	20.67	21.0	3.48	0.84		C	f
	$^2P_{1/2}$–$^2P^o_{1/2}$	2979.05	22.0	1.00	25.2	29.7	3.93	0.75		C+	c
			22.0	1.00	59.17	29.7	3.93	1.76		A	f
	$^2P_{3/2}$–$^2P^o_{1/2}$	2891.61	22.0	1.00	23.6	27.9	3.69	0.75		C+	c
			22.0	1.00	54.24	27.9	3.69	1.72		A	f
	$^2P_{1/2}$–$^2P^o_{3/2}$	3033.51	26.0	1.76	32.0	45.8	6.97	0.61		B	a
			22.0	1.00	21.2	27.5	3.90	0.68		B	c
			22.0	1.00	35.18	27.5	3.90	1.12		A	f
	$^2P_{3/2}$–$^2P^o_{3/2}$	2942.89	26.0	1.76	34.4	43.1	6.60	0.69		B	a
			22.0	1.00	20.2	25.8	3.66	0.69		C+	c
			22.0	1.00	33.48	25.8	3.66	1.14		B	f
(^{1}D) 4s–(^{1}D) 4p	$^2D_{5/2}$–$^2F^o_{7/2}$	4609.57	10.88	2.03	49.1	113	13.3	0.39		B+	b
			11.52	1.79	46.6	99.8	11.9	0.42		B+	b
			12.20	0.74	21.4	41.3	5.04	0.46		A	b
			13.03	1.10	26.9	61.4	7.43	0.39		A	b
			13.88	1.39	36.2	77.6	9.32	0.42		B+	b
			22.0	1.00	34.0	42.6	7.67	0.68		B	c
			17.0–26.7	1.00	30.2	47.0–40.1	7.39–7.83	0.56–0.63		B+	d
			13.4	1.30	56.0	66.7	9.16	0.74		B+	g
			14.2	1.60	62.0	80.3	11.3	0.68		B+	g
	$^2D_{3/2}$–$^2F^o_{5/2}$	4589.90	10.88	2.03	53.3	110	13.2	0.43		B+	b
			11.52	1.79	45.9	96.6	11.7	0.42		B+	b
			12.20	0.74	25.9	39.9	4.98	0.58		A	b
			13.03	1.10	32.4	59.3	7.33	0.49		A	b
			13.88	1.39	39.0	75.0	9.20	0.46		B+	b
			22.0	1.00	35.0	40.9	7.58	0.72		B+	c
			16.5–23.2	1.00	29.8	45.8–40.6	7.25–7.63	0.56–0.62		B	d
	$^2D_{5/2}$–$^2F^o_{5/2}$	4637.23	22.0	1.00	36.5	43.0	7.70	0.72		B	c
			18.4–26.5	1.00	36.6	45.9–40.6	7.52–7.86	0.69–0.76		B	d
	$^2D_{5/2}$–$^2P^o_{3/2}$	4277.53	26.0	1.76	85.2	85.86	13.9	0.85		B	a
			22.0	1.00	72.1	51.7	7.74	1.21		B	c
	$^2D_{3/2}$–$^2P^o_{3/2}$	4237.22	18.4–26.5	1.00	57.9	53.3–47.0	7.38–7.82	0.95–1.06		B+	d
	$^2D_{3/2}$–$^2D^o_{3/2}$	4042.89	22.0	1.00	27.7	36.8	6.62	0.64		B	c
			18.4–26.5	1.00	41.4	39.2–34.6	6.47–6.72	0.91–1.00		B+	d
			22.0	1.00	29.27	36.8	6.62	0.68		C	f
	$^2D_{5/2}$–$^2D^o_{3/2}$	4079.57	18.4–26.5	1.00	42.9	40.8–36.0	6.60–6.87	0.91–1.00		B+	c
	$^2D_{3/2}$–$^2D^o_{5/2}$	4035.46	22.0	1.00	29.1	33.3	6.61	0.73		B	c
			18.4–26.5	1.00	36.7	35.6–31.2	6.46–6.72	0.85–0.97		B+	d
			22.0	1.00	31.73	33.3	6.61	0.80		B	f
(^{3}P) 4p–(^{3}P) 4d	$^4P^o_{3/2}$–$^4D_{5/2}$	3514.39	22.0	1.00	46.0	43.9	6.48	0.91		C+	c
			22.0	1.00	49.93	43.9	6.48	0.99		B	f
	$^4P^o_{1/2}$–$^4D_{3/2}$	3535.32	22.0	1.00	52.0	45.2	6.62	1.00		C+	c
			22.0	1.00	48.52	45.2	6.62	0.94		A	f
	$^4P^o_{5/2}$–$^4D_{5/2}$	3476.75	26.0	1.76	62.4	73.5	11.3	0.74		B	a
			22.0	1.00	35.4	42.8	6.32	0.72		C+	c
			22.0	1.00	46.18	42.8	6.32	0.94		C	f
	$^4P^o_{1/2}$–$^4D_{1/2}$	3509.78	22.0	1.00	38.0	45.0	6.57	0.74		C+	c
			22.0	1.00	46.82	45.0	6.57	0.91		A	f
	$^4P^o_{5/2}$–$^4D_{3/2}$	3454.09	22.0	1.00	45.9	43.1	6.29	0.93		B	f
	$^4P^o_{5/2}$–$^4P_{5/2}$	3139.02	22.0	1.00	35.6	40.5	6.15	0.76	45.6	C+	c
			22.0	1.00	45.27	40.5	6.15	0.97	45.6	B	f
	$^4P^o_{3/2}$–$^4P_{3/2}$	3212.52	22.0	1.00	36.6	43.0	6.34	0.74	47.5	C+	c
			22.0	1.00	48.91	43.0	6.34	0.99	47.5	A	f
	$^4P^o_{1/2}$–$^4P_{1/2}$	3281.71	22.0	1.00	41.8	46.3	6.67	0.79	49.8	C+	c
			22.0	1.00	51.30	46.3	6.67	0.97	49.8	A	f

Table 1 – *continued*

Transition array	Transition	λ (Å)	T (10^3 K)	N_e (10^{17} cm^{-3})	W_m (pm)	W_e (pm)	W_i (pm)	W_m/W	W_G (pm)	Acc.	Ref.
	$^4P^o_{5/2}$–$^4P_{3/2}$	3181.04	22.0	1.00	35.0	42.0	6.22	0.73	47.3	C+	c
			22.0	1.00	53.21	42.0	6.22	1.10	47.3	A	f
	$^4P^o_{3/2}$–$^4P_{1/2}$	3243.69	22.0	1.00	36.8	45.4	6.51	0.71	48.4	C+	c
			22.0	1.00	47.32	45.4	6.51	0.91	48.4	B	f
	$^4P^o_{1/2}$–$^4P_{3/2}$	3249.80	26.0	1.76	66.4	77.1	–	0.86	85.1	B	a
			22.0	1.00	36.6	43.8	6.51	0.73	48.8	B	c
			22.0	1.00	48.54	43.8	6.51	0.96	48.8	B	f
	$^4P^o_{3/2}$–$^4P_{5/2}$	3169.67	26.0	1.76	66.4	71.2	–	0.93	81.0	B	a
			22.0	1.00	35.6	41.5	6.28	0.76	46.2	B	c
			22.0	1.00	44.25	41.5	6.28	0.93	46.2	B	f
	$^4P^o_{5/2}$–$^4F_{3/2}$	3194.23	22.0	1.00	48.27	40.6	6.07	1.03		A	f
	$^4P^o_{5/2}$–$^4F_{5/2}$	3221.63	22.0	1.00	39.54	41.6	6.14	0.83		C	f
	$^4P^o_{3/2}$–$^4F_{3/2}$	3225.97	22.0	1.00	42.51	41.6	6.20	0.89		B	f
	$^4P^o_{1/2}$–$^4F_{3/2}$	3263.57	22.0	1.00	48.80	42.4	6.35	1.00		A	f
	$^4D^o_{7/2}$–$^4D_{7/2}$	3780.84	26.0	1.76	81.6	87.6	13.4	0.81	96.0	B	a
			22.0	1.00	57.7	52.3	7.54	0.96	55.5	B	c
			18.4–26.5	1.00	75.4	53.0–49.7	7.33–7.70	1.26–1.31	56.3–54.6	B+	d
			22.0	1.00	51.12	52.3	7.54	0.85	55.5	B	f
	$^4D^o_{5/2}$–$^4D_{5/2}$	3826.81	22.0	1.00	67.7	53.5	7.79	1.11	56.9	B	c
			18.4–26.5	1.00	64.3	55.4–52.0	7.57–7.97	1.02–1.07	57.4–55.9	B+	d
			22.0	1.00	53.78	53.5	7.79	0.88	56.9	A	f
	$^4D^o_{3/2}$–$^4D_{3/2}$	3872.14	22.0	1.00	53.5	55.2	8.02	0.85	58.2	B	c
			18.4–26.5	1.00	76.7	57.2–53.7	7.85–8.21	1.18–1.24	59.0–57.2	B+	d
	$^4D^o_{1/2}$–$^4D_{1/2}$	3880.33	18.4–26.5	1.00	53.5	58.7–54.8	8.01–8.28	0.80–0.85	59.4–57.5	B+	d
			22.0	1.00	50.36	56.5	8.14	0.78	45.3	B	f
	$^4D^o_{7/2}$–$^4D_{5/2}$	3763.50	18.4–26.5	1.00	56.2	53.02–49.7	7.27–7.68	0.93–0.98	55.6–56.2	B+	d
			22.0	1.00	55.23	51.13	7.49	0.94	56.9	A	f
	$^4D^o_{5/2}$–$^4D_{3/2}$	3799.38	22.0	1.00	48.5	53.7	7.74	0.79	56.4	B	c
			18.4–26.5	1.00	56.9	55.8–52.3	7.59–7.91	0.90–0.95	56.9–55.2	B+	d
			22.0	1.00	54.97	53.7	7.74	0.89	56.4	A	f
	$^4D^o_{3/2}$–$^4D_{1/2}$	3841.52	22.0	1.00	44.4	54.9	8.03	0.71	57.7	B	c
			18.4–26.5	1.00	48.1	56.8–53.3	7.76–8.37	0.75–0.78	58.0–64.1	B+	d
			22.0	1.00	48.23	54.9	8.03	0.77	57.7	A	f
	$^4D^o_{5/2}$–$^4D_{7/2}$	3844.73	22.0	1.00	20.0	53.7	7.82	0.33	57.1	C+	c
			22.0	1.00	59.14	53.7	7.82	0.96	57.1	B	f
	$^4D^o_{3/2}$–$^4D_{5/2}$	3900.63	18.4–26.5	1.00	52.2	56.7–53.2	7.76–8.37	0.81–0.85	59.3–52.5	B+	d
			22.0	1.00	55.47	54.81	8.07	0.88	56.6	B	f
	$^4D^o_{1/2}$–$^4D_{3/2}$	3911.58	18.4–26.5	1.00	47.8	59.1–55.3	8.05–8.41	0.72–075	60.5–58.3	B+	d
			22.0	1.00	51.42	56.9	8.22	0.79	57.1	A	f
	$^4D^o_{7/2}$–$^4F_{9/2}$	3588.44	26.0	1.76	88.2	91.0	–	0.97		B	a
			11.52	1.79	84.2	115	–	0.73		B+	b
			13.03	1.10	54.0	71.6	–	0.75		A	b
			13.88	1.39	64.2	82.4	–	0.78		B+	b
			22.0	1.00	59.6	53.0	7.43	0.99		B	c
	$^4D^o_{5/2}$–$^4F_{7/2}$	3576.62	26.0	1.76	104.2	91.5	–	1.14		C+	a
			22.0	1.00	62.3	53.3	7.59	1.02		B	c
			18.4–26.5	1.00	118.0	55.0–51.9	7.45–7.74	1.89–1.98		C+	d
	$^4D^o_{3/2}$–$^4F_{5/2}$	3582.35	22.0	1.00	65.6	52.5	7.72	1.09		B	c
	$^4D^o_{1/2}$–$^4F_{3/2}$	3581.61	22.0	1.00	51.3	52.5	7.74	0.85		B	c
	$^4D^o_{5/2}$–$^4F_{5/2}$	3519.99	22.0	1.00	55.67	51.1	7.43	0.95		B	f
	$^4D^o_{3/2}$–$^4F_{3/2}$	3548.51	22.0	1.00	54.27	51.1	7.59	0.92		C	f
	$^4D^o_{1/2}$–$^4P_{3/2}$	3565.03	26.0	1.76	100.4	92.7	–	1.08		B	a
			22.0	1.00	57.0	54.2	7.92	0.92		C+	c
	$^4D^o_{7/2}$–$^4P_{5/2}$	3370.91	22.0	1.00	54.76	47.6	7.14	1.00		A	f
	$^4D^o_{5/2}$–$^4P_{5/2}$	3421.61	22.0	1.00	58.28	49.5	7.39	1.02		A	f
	$^4D^o_{3/2}$–$^2F_{5/2}$	3397.90	22.0	1.00	60.57	55.1	8.06	0.96		A	f
	$^4D^o_{5/2}$–$^2F_{7/2}$	3430.42	22.0	1.00	63.28	57.4	7.99	0.97		A	f
	$^4D^o_{5/2}$–$^2D_{5/2}$	2865.84	22.0	1.00	69.64	66.5	–	1.05		A	f
	$^2D^o_{5/2}$–$^4D_{3/2}$	3958.38	22.0	1.00	12.0	60.6	8.44	0.17		C+	c
			22.0	1.00	62.43	60.6	8.44	0.90		A	f
	$^2D^o_{5/2}$–$^4D_{5/2}$	3988.16	22.0	1.00	58.0	60.5	8.52	0.84		B	c

Table 1 – *continued*

Transition array	Transition	λ (Å)	T (10^3 K)	N_e (10^{17} cm^{-3})	W_m (pm)	W_e (pm)	W_i (pm)	W_m/W	W_G (pm)	Acc.	Ref.
			18.4–26.5	1.00	68.2	62.7–58.7	8.34–8.72	0.96–1.01		B+	d
			22.0	1.00	59.38	60.5	8.52	0.86		B	f
	$^2D^o_{3/2}$–$^4D_{1/2}$	4031.38	22.0	1.00	57.66	64.4	8.98	0.79		C	f
	$^2D^o_{3/2}$–$^2D_{3/2}$	3000.44	22.0	1.00	88.0	73.5	–	1.20		C+	c
	$^2D^o_{5/2}$–$^2D_{5/2}$	2955.39	22.0	1.00	69.6	72.0	–	0.97		C+	c
			22.0	1.00	79.10	72.0	–	1.10		A	f
	$^2D^o_{3/2}$–$^2D_{5/2}$	3014.48	22.0	1.00	69.8	75.2	–	0.93		C+	c
			22.0	1.00	83.62	75.2	–	1.11		A	f
	$^2D^o_{5/2}$–$^2F_{7/2}$	3559.51	22.0	1.00	67.7	63.8	8.65	0.93	67.0	B	c
	$^2D^o_{5/2}$–$^2F_{5/2}$	3464.13	26.0	1.76	100.4	102	–	0.98	111.6	B	a
			22.0	1.00	58.5	59.5	8.38	0.86	64.3	C+	c
			22.0	1.00	64.07	59.5	8.38	0.94	64.3	B	f
	$^2D^o_{3/2}$–$^2F_{5/2}$	3545.60	22.0	1.00	66.67	62.7	6.66	0.96	64.1	C	f
	$^2D^o_{3/2}$–$^2P_{1/2}$	3273.32	22.0	1.00	78.0	70.61	–	1.10		C+	c
			22.0	1.00	90.79	70.61	–	1.28		A	f
	$^2D^o_{3/2}$–$^2P_{3/2}$	3204.32	22.0	1.00	104.18	73.1	–	1.42		A	f
	$^2P^o_{3/2}$–$^2F_{5/2}$	3655.28	22.0	1.00	63.0	63.7	9.34	0.86		C+	c
			18.4–26.5	1.00	85.5	65.5–62.1	9.07–9.49	1.15–1.19		B+	d
			22.0	1.00	67.72	63.7	9.34	0.93		C	f
	$^2P^o_{1/2}$–$^2P_{1/2}$	3307.23	26.0	1.76	132.6	118	–	1.12	221	B	a
			22.0	1.00	93.07	68.5	–	1.36	124.1	A	f
	$^2P^o_{1/2}$–$^2P_{3/2}$	3236.81	22.0	1.00	75.6	72.3	–	1.05	120	C+	c
			22.0	1.00	93.27	72.3	–	1.29	120	A	f
	$^2P^o_{3/2}$–$^2P_{1/2}$	3366.58	22.0	1.00	94.78	70.9	–	1.34		A	f
	$^2P^o_{3/2}$–$^2D_{5/2}$	3093.40	22.0	1.00	69.7	77.5	–	0.90		C+	c
			22.0	1.00	88.77	77.5	–	1.15		A	f
	$^2P^o_{1/2}$–$^2D_{3/2}$	3028.91	22.0	1.00	77.92	73.1	–	1.07		B	f
	$^4S^o_{3/2}$–$^4F_{3/2}$	3952.73	22.0	1.00	58.9	62.6	9.56	0.82		C+	c
			18.4–26.5	1.00	69.8	64.6–60.7	9.36–9.77	0.94–0.99		B+	d
			22.0	1.00	70.09	62.6	9.56	0.97		A	f
	$^4S^o_{3/2}$–$^4P_{5/2}$	3868.53	26.0	1.76	115.4	106	–	1.09	121.5	B	a
			22.0	1.00	78.7	61.8	9.59	1.10	69.6	B	c
			18.4–26.5	1.00	72.6	63.8–59.9	9.38–9.77	0.99–1.04	70.5–69.1	B	d
			22.0	1.00	69.45	61.8	9.59	0.97	69.6	B	f
	$^4S^o_{3/2}$–$^4P_{3/2}$	3932.55	22.0	1.00	80.4	64.2	9.38	1.09	71.8	B	c
			18.4–26.5	1.00	85.7	66.6–62.4	9.53–9.96	1.13–1.18	72.6–71.4	B+	d
			22.0	1.00	72.00	64.2	9.38	0.98	71.8	B	f
	$^4S^o_{3/2}$–$^4P_{1/2}$	3979.36	22.0	1.00	79.5	68.6	10.06	1.01	73.6	B	c
			18.4–26.5	1.00	83.6	70.7–66.6	9.66–10.17	1.04–1.09	74.6–72.7	B+	d
	$^2S^o_{1/2}$–$^2P_{3/2}$	3388.53	26.0	1.76	134.2	137	–	0.98		B	a
	$^2S^o_{1/2}$–$^2D_{3/2}$	3161.37	22.0	1.00	74.66	80.4	–	0.93		B	f
(^{3}P) 4p–(^{1}D) 4d	$^2P^o_{3/2}$–$^2P_{3/2}$	2544.68	22.0	1.00	42.6	71.7	–	0.59		C+	c
(^{1}D) 4p–(^{3}P) 4d	$^2D^o_{5/2}$–$^2D_{5/2}$	5216.81	18.4–26.5	1.00	252.7	240–224	–	1.05–1.13		A	d
	$^2D^o_{5/2}$–$^2P_{3/2}$	5812.76	18.4–26.5	1.00	291.1	260–241	–	1.12–1.21		B+	d
(^{1}D) 4p–(^{1}D) 4d	$^2F^o_{7/2}$–$^2G_{9/2}$	3561.03	22.0	1.00	63.9	64.2	–	1.00		B	c
			22.0	1.00	57.43	64.2	–	0.89		C	f
	$^2F^o_{7/2}$–$^2F_{7/2}$	3376.44	26.0	1.76	117.4	158	–	0.74		B	a
			22.0	1.00	66.8	92.6	–	0.72		C+	c
			22.0	1.00	83.92	92.6	–	0.91		A	f
	$^2F^o_{5/2}$–$^2F_{5/2}$	3350.92	22.0	1.00	59.1	95.6	–	0.62		B	c
			22.0	1.00	67.96	95.6	–	0.71		A	f
	$^2F^o_{7/2}$–$^2F_{5/2}$	3365.52	22.0	1.00	66.49	95.8	–	0.70		A	f
	$^2F^o_{5/2}$–$^2D_{5/2}$	3414.46	22.0	1.00	67.05	101	–	0.66		B	f
	$^2P^o_{3/2}$–$^2P_{3/2}$	3660.44	18.4–26.5	1.00	123.6	164–155	–	0.75–0.80		B+	d
			22.0	1.00	115.78	159	–	0.73		A	f
	$^2P^o_{3/2}$–$^2P_{1/2}$	3671.00	22.0	1.00	110.39	158	–	0.70		C	f
	$^2P^o_{1/2}$–$^2P_{1/2}$	3754.05	22.0	1.00	122.39	166	–	0.74		A	f
	$^2P^o_{3/2}$–$^2D_{5/2}$	3639.83	22.0	1.00	21.6	124	–	0.174		B	c

Table 1 – *continued*

Transition array	Transition	λ (Å)	T (10^3 K)	N_e (10^{17} cm^{-3})	W_m (pm)	W_e (pm)	W_i (pm)	W_m/W	W_G (pm)	Acc.	Ref.
			22.0	1.00	110.33	124	–	0.89		A	f
	$^2P^o_{1/2}$–$^2D_{3/2}$	3680.06	22.0	1.00	142.41	121	–	1.18		B	f
	$^2P^o_{3/2}$–$^2S_{1/2}$	3026.75	22.0	1.00	110.85	128	–	0.87		A	f
	$^2P^o_{1/2}$–$^2S_{1/2}$	3082.98	22.0	1.00	119.74	134	–	0.89		B	f
	$^2D^o_{5/2}$–$^2P_{3/2}$	3825.67	22.0	1.00	105.4	168	–	0.63		C+	c
			22.0	1.00	100.13	168	–	0.60		C	f
	$^2D^o_{3/2}$–$^2P_{3/2}$	3819.02	18.4–26.5	1.00	136.1	173–162	–	0.79–0.84		B+	d
			22.0	1.00	95.29	167	–	0.57		B	f
	$^2D^o_{3/2}$–$^2P_{1/2}$	3830.52	22.0	1.00	113.88	163	–	0.70		C	f
	$^2D^o_{5/2}$–$^2D_{5/2}$	3803.17	26.0	1.76	69.0	217	–	0.32		C	a
			22.0	1.00	100.7	126	–	0.80		B	c
			18.4–26.5	1.00	113.4	130–124	–	0.87–0.91		B	d
			22.0	1.00	108.62	126	–	0.86		B	f
	$^2D^o_{3/2}$–$^2D_{5/2}$	3796.59	18.4–26.5	1.00	100.0	132–125	–	0.76–0.80		B+	d
			22.0	1.00	101.68	128	–	0.79		B	f
	$^2D^o_{5/2}$–$^2F_{7/2}$	3737.89	26.0	1.76	145.6	196	–	0.74		B	a
			22.0	1.00	101.2	115	–	0.88		B	c
			18.4–26.5	1.00	112.6	118–111	–	0.95–1.01		A	d
			22.0	1.00	91.44	115	–	0.80		B	f
	$^2D^o_{3/2}$–$^2F_{5/2}$	3718.21	22.0	1.00	96.1	121	–	0.79		B	c
			18.4–26.5	1.00	93.2	124–117	–	0.75–0.80		B+	d
			22.0	1.00	84.72	121	–	0.70		B	f
	$^2D^o_{5/2}$–$^2F_{5/2}$	3724.52	18.4–26.5	1.00	114.4	123–115	–	0.93–0.99		B+	d
(^{3}P) 4p–(^{3}P) 5s	$^4P^o_{5/2}$–$^4P_{5/2}$	3765.27	18.4–26.5	1.00	74.2	59.3–55.0	4.67–5.18	1.16–1.23	67.5–66.25	B+	d
			22.0	1.00	62.63	56.9	4.91	1.01	63.9	B	f
	$^4P^o_{3/2}$–$^4P_{3/2}$	3720.43	22.0	1.00	61.6	56.5	4.85	1.00	65.5	C+	c
			18.4–26.5	1.00	84.2	58.9–54.4	4.60–5.08	1.32–1.41	65.8–64.8	B+	d
			22.0	1.00	63.67	56.5	4.85	1.04	65.5	C	f
	$^4P^o_{3/2}$–$^4P_{1/2}$	3622.14	22.0	1.00	66.2	54.1	4.58	1.12	62.5	B	c
			18.4–26.5	1.00	80.2	56.5–52.2	4.35–4.79	1.32–1.41	62.7–61.7	B+	d
			22.0	1.00	68.4	54.1	4.58	1.17	62.5	A	f
	$^4P^o_{3/2}$–$^4P_{5/2}$	3809.46	22.0	1.00	74.6	58.6	5.05	1.17	69.1	B	c
			18.4–26.5	1.00	75.3	61.0–56.6	4.80–5.30	1.14–1.22	69.1–67.8	B+	d
			22.0	1.00	68.70	58.6	5.05	1.08	69.1	A	f
	$^4P^o_{1/2}$–$^4P_{3/2}$	3770.52	18.4–26.5	1.00	76.7	60.4–55.8	4.74–5.23	1.18–1.26	67.9–66.7	B+	d
			22.0	1.00	68.64	57.9	4.98	1.09	64.1	B	f
	$^4P^o_{1/2}$–$^4P_{1/2}$	3669.60	22.0	1.00	62.74	55.3	4.71	1.05	60.9	B	f
	$^4P^o_{5/2}$–$^4P_{3/2}$	3678.27	22.0	1.00	67.08	55.1	4.73	1.12	61.5	B	f
	$^4P^o_{1/2}$–$^2P_{3/2}$	3650.89	22.0	1.00	69.48	53.5	4.54	1.20		A	f
	$^4D^o_{3/2}$–$^4P_{1/2}$	4033.81	22.0	1.00	83.0	68.2	5.87	1.12		B	c
			18.4–26.5	1.00	88.4	71.2–65.8	5.58–6.14	1.15–1.23		B+	d
			22.0	1.00	89.75	68.2	5.87	1.21		B	f
	$^4D^o_{5/2}$–$^4P_{5/2}$	4179.30	18.4–26.5	1.00	86.4	75.9–70.5	5.99–6.57	1.06–1.12		B+	d
	$^4D^o_{3/2}$–$^4P_{3/2}$	4156.08	18.4–26.5	1.00	83.3	74.7–69.0	5.88–6.49	1.03–1.10		B+	d
	$^4D^o_{3/2}$–$^2P_{3/2}$	4011.21	18.4–26.5	1.00	90.5	67.8–62.9	5.27–5.83	1.24–1.32		B+	d
			22.0	1.00	82.16	65.1	5.25	1.17		B	f
	$^2D^o_{3/2}$–$^2P_{3/2}$	4218.66	22.0	1.00	84.9	75.8	6.42	1.03	88.4	B	c
			18.4–26.5	1.00	90.3	79.1–73.0	6.10–6.71	1.06–1.13	88.6–87.7	A	d
	$^2P^o_{3/2}$–$^2P_{1/2}$	4222.64	22.0	1.00	82.0	73.4	6.43	1.03		B	c
			18.4–26.5	1.00	90.3	76.3–70.9	6.16–6.80	1.10–1.16		A	d
	$^2P^o_{1/2}$–$^2P_{3/2}$	4275.16	22.0	1.00	60.8	73.2	6.51	0.76		B	c
	$^4S^o_{3/2}$–$^4P_{5/2}$	4865.91	18.4–26.5	1.00	128.5	101–93.3	8.21–9.02	1.17–1.26		B+	d
	$^4S^o_{3/2}$–$^2P_{3/2}$	4535.49	18.4–26.5	1.00	106.2	85.1–76.6	6.97–7.66	1.15–1.26		B+	d
(^{3}P) 4p–(^{1}D) 5s	$^2P^o_{1/2}$–$^2D_{3/2}$	2764.65	22.0	1.00	34.37	29.6	2.75	1.06		B	f
(^{1}D) 4p–(^{1}D) 5s	$^2F^o_{7/2}$–$^2D_{5/2}$	3946.10	22.0	1.00	91.8	68.1	7.04	1.22		B	c
			18.4–26.5	1.00	81.1	71.3–65.2	6.84–7.29	1.04–1.12		B+	d
			22.0	1.00	74.86	68.1	7.04	1.00		B	f
	$^2F^o_{5/2}$–$^2D_{3/2}$	3925.72	26.0	1.76	145.4	107	12.5	1.21		B	a

Table 1 – *continued*

Transition array	Transition	λ (Å)	T (10^3 K)	N_e (10^{17} cm^{-3})	W_m (pm)	W_e (pm)	W_i (pm)	W_m/W	W_G (pm)	Acc.	Ref.
			22.0	1.00	78.5	63.4	6.90	1.17		B	c
			18.4–26.5	1.00	94.1	66.5–60.7	6.69–7.17	1.29–1.39		B+	d
			22.0	1.00	74.73	63.4	6.90	1.06		B	f
	$^2F^o_{5/2}$–$^2D_{5/2}$	3926.05	22.0	1.00	68.65	63.7	6.94	0.97		C	f
(^{1}S) 4s–(^{3}P) 5p	$^2S_{1/2}$–$^2D^o_{3/2}$	4217.43	22.0	1.00	73.4	91.3	–	0.80		C+	c
			18.4–26.5	1.00	100.8	93.0–89.5	–	1.08–1.13		B+	d
	$^2S_{1/2}$–$^4D^o_{3/2}$	4385.06	18.4–26.5	1.00	96.9	93.6–89.0	–	1.03–1.09		B+	d
	$^2S_{1/2}$–$^4S^o_{3/2}$	4189.65	18.4–26.5	1.00	104.1	85.9–82.0	–	1.21–1.27		B+	d
(^{1}D) 3d–(^{1}D) 4p	$^2G_{9/2}$–$^2F^o_{7/2}$	6114.92	22.0	1.00	55.1	64.7	14.5	0.70		B	c
			18.4–26.5	1.00	34.7	68.9–60.84	14.1–14.6	0.42–0.46		B+	d
	$^2G_{7/2}$–$^2F^o_{7/2}$	6123.36	22.0	1.00	57.4	64.9	14.6	0.72		B	c
	$^2G_{7/2}$–$^2F^o_{5/2}$	6172.29	18.4–26.5	1.00	47.7	71.8–63.9	14.3–14.9	0.55–0.61		B+	d

In the first five columns of Table 1, we give the transition array, transition, wavelength, electron temperature (T) and electron density (N_e). In column 6 of Table 1, we show the experimental Stark widths (W_m). In columns 7 and 8, we present our electron-impact Stark widths (W_e) and ion impact Stark widths (W_i) calculated using the SCP approach as described in Section 2. Ionic perturbers are Ar^+ ions. The ratios (W_m/W) between the experimental and our calculated Stark widths are shown in column 9, where $W = W_e + W_i$ is the total width. In column 10, we present the Stark widths of Griem (1974). The accuracies of the experimental results are presented in column 11. We use code letters from critical reviews of Konjević et al. (2002), which indicate the following:

(i) A = uncertainties within 15 per cent
(ii) B+ = uncertainties within 23 per cent
(iii) B = uncertainties within 30 per cent
(iv) C+ = uncertainties within 40 per cent
(v) C = uncertainties within 50 per cent
(vi) D = uncertainties larger than 50 per cent

Finally, in the last column of Table 1, a label for each set of experimental results is given.

For each value in Table 1, the collision volume (V) multiplied by the perturber density is much less than 1 and the impact approximation is valid. If the impact approximation is not valid, the values of the width are not given. For example, for the transition (^{3}P) 4p $^4P^o_{1/2}$–(^{3}P) 4d $^4P_{3/2}$ (λ = 3249.80 Å), we do not give the value of the ion impact Stark width when we compare with Djeniže et al. (1989).

We found that our Stark widths agree well with the experimental results for the (^{3}P) 3d–(^{3}P) 4p transitions (Hamdi et al. 2017). For example, the average agreement with Aparicio et al. (1998), Iglesias et al. (2006) and Djurović et al. (2013) is about 20 per cent. In Fig. 1, we present our electron-impact Stark width as a function of temperature for the interval from 5000 to 60 000 K along with the experimental values of Pellerin et al. (1997), Aparicio et al. (1998) and Iglesias et al. (2006) for the transition (^{3}P) 3d $^4D_{5/2}$–(^{3}P) 4p $^4D^o_{5/2}$ (λ = 3968.36 Å). All experimental results are normalized to an electron density of 10^{17} cm^{-3}. Fig. 1 shows that our Stark widths are close to the result of Pellerin et al. (1997) and the results of Iglesias et al. (2006) measured at the electron densities 4.50 × 10^{17} cm^{-3} and 9.00 × 10^{17} cm^{-3}. These last two results give the same value after normalization. Fig. 1 shows also that our electron-impact Stark widths underestimate the value of Aparicio et al. (1998) and overestimate the value of Iglesias et al. (2006) measured at the electron densities 7.20 × 10^{17} cm^{-3}.

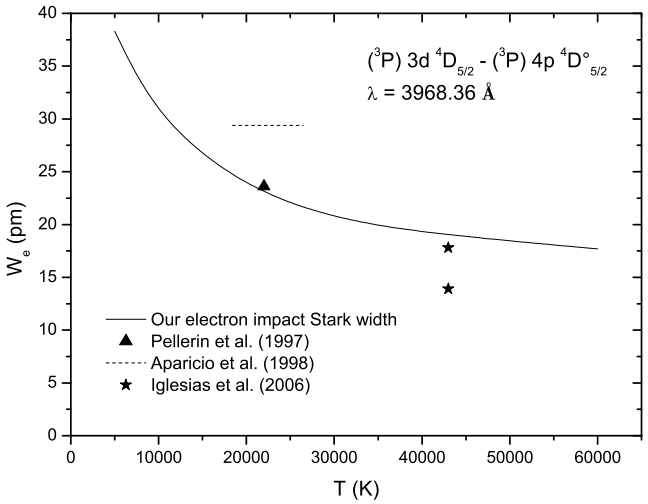

Figure 1. Electron-impact (Stark) FWHM obtained using the SCP approach (Sahal-Bréchot 1969a,b) for the (^{3}P) 3d $^4D_{5/2}$–(^{3}P) 4p $^4D^o_{5/2}$ (λ = 3968.36 Å) spectral line as a function of electron temperature compared with experimental results. The electron density is 10^{17} cm^{-3}.

For the (^{3}P) 3d–(^{1}D) 4p transition array, the agreement with experiments is worse than for the (^{3}P) 3d–(^{3}P) 4p transitions. The average difference with Pellerin et al. (1997) is 44 per cent. Compared with Aparicio et al. (1998), the difference does not exceed 44 per cent for eight transitions. For three transitions, the agreement is poor. The best agreement with Aparicio et al. (1998) is for the transition $^2F_{5/2}$–$^2D^o_{5/2}$ (λ = 4300.65 Å) for which the ratio W_m/W varies from 0.98 to 1.08 in the temperature interval from 18 400 to 26 500 K. The largest difference with Aparicio et al. (1998) is for the transition $^2P_{3/2}$–$^2P^o_{3/2}$ (λ = 3766.12 Å) for which our width is two orders of magnitude lower than the experimental result. Compared with Djurović et al. (2013), we find very good agreement (which does not exceed 22 per cent). On one hand, for the transition

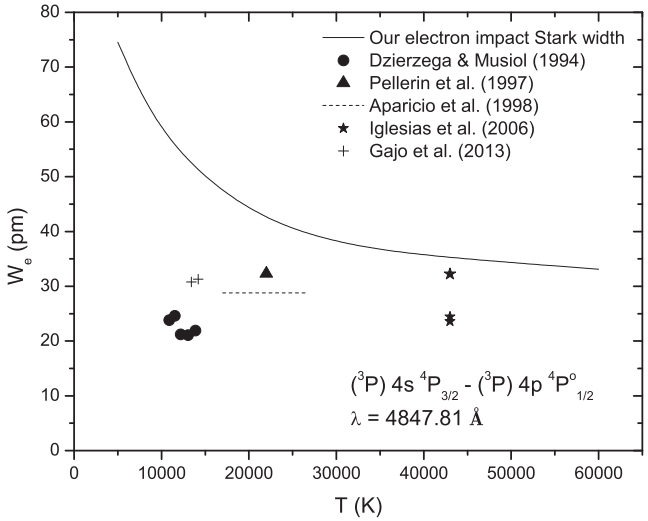

Figure 2. Same as Fig. 1 but for the (^3P) 4s $^4P_{3/2}$–(^3P) 4p $^4P^o_{1/2}$ ($\lambda = 4847.81$ Å) spectral line.

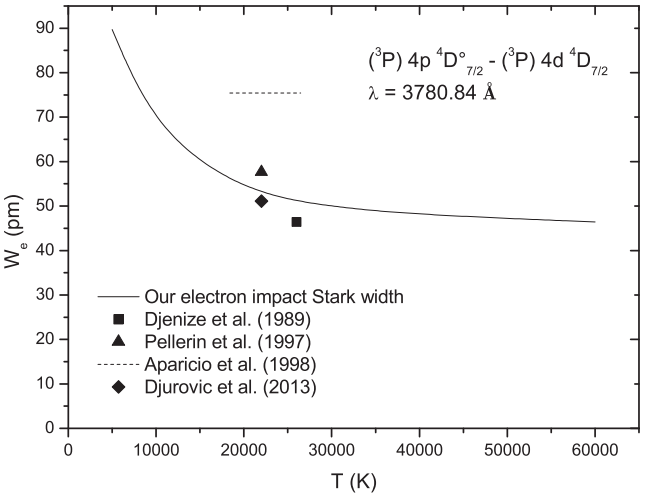

Figure 3. Same as Fig. 1 but for the (^3P) 4p $^4D^o_{7/2}$–(^3P) 4d $^4D_{7/2}$ ($\lambda = 3780.84$ Å) spectral line.

$^2D_{5/2}$–$^2D^o_{5/2}$ ($\lambda = 4481.81$ Å), our widths are two orders of magnitude greater than the experimental results of Dzierzega & Musiol (1994). On the other hand, the agreement is good with Pellerin et al. (1997) ($W_m/W = 0.75$).

For the (^3P) 4s–(^3P) 4p transition array, we found an average difference with Pellerin et al. (1997) of 30 per cent. Better agreement is found for the transition $^4P_{5/2}$–$^4D^o_{3/2}$ ($W_m/W = 0.92$). The largest difference is 75 per cent, which was obtained for the transition $^4P_{3/2}$–$^2D^o_{3/2}$ ($\lambda = 4112.82$ Å). Compared with Aparicio et al. (1998), the average difference is about 40 per cent. All the values of Aparicio et al. (1998) are measured with uncertainties within 23 per cent. The largest disagreement with Aparicio et al. (1998) is for the $^2P_{3/2}$–$^4D^o_{5/2}$ ($\lambda = 5145.31$ Å) spectral line. In fact, for this line, the ratio W_m/W varies from 0.40 to 0.43 in the temperature interval from 18 400 to 26 500 K. Note for this line that the ratio W_m/W is 0.77 when we compare with Pellerin et al. (1997). Comparing with Gajo et al. (2013), we found the average of W_m/W was 0.70. All our values overestimate the experimental widths of Gajo et al. (2013). Our results agree with the widths of Iglesias et al. (2006) within 25 per cent on average. The largest disagreement ($W_m/W = 0.59$) was for the transition $^4P_{3/2}$–$^4P^o_{1/2}$ ($\lambda = 4847.81$ Å) for the width measured at the electron density 7.20×10^{17} cm^{-3}. However, for the width measured at the electron density 9.00×10^{17} cm^{-3}, the ratio W_m/W is 0.80. Our widths do not agree with Dzierzega & Musiol (1994) for all transitions in the (^3P) 4s–(^3P) 4p transition array. In fact, our widths are two orders of magnitude greater than the results of Dzierzega & Musiol (1994). Our results agree with Griem (1974) within 25 per cent on average. In Fig. 2, we present our electron-impact Stark width as a function of temperature for the interval from 5000 to 60 000 K along with the experimental values of Dzierzega & Musiol (1994), Pellerin et al. (1997), Aparicio et al. (1998), Iglesias et al. (2006) and Gajo et al. (2013) for the transition (^3P) 4s $^4P_{3/2}$–(^3P) 4p $^4P^o_{1/2}$ ($\lambda = 4847.81$ Å). As we can see in Fig. 2, our results overestimate all the experimental results. The value of Iglesias et al. (2006) measured at the electron density 9.00×10^{17} cm^{-3} is the closest to our width.

For the (^3P) 4s–(^1D) 4p transition array, our widths agree with Pellerin et al. (1997) within 47 per cent on average and with Djeniže et al. (1989) within 54 per cent. Good agreement was found when we compare with Djurović et al. (2013) except for two transitions: $^2P_{1/2}$–$^2P^o_{1/2}$ ($\lambda = 2979.05$ Å) and $^2P_{3/2}$–$^2P^o_{1/2}$ ($\lambda = 2891.61$ Å), for which the ratio W_m/W is 1.76 and 1.72, respectively. For the same lines, the ratio W_m/W is 0.75 when we compare with Pellerin et al. (1997).

For the (^1D) 4s–(^1D) 4p transition array, the agreement with Pellerin et al. (1997) is 39 per cent on average and 28 per cent with Aparicio et al. (1998). The largest disagreement was with Dzierzega & Musiol (1994).

For the (^3P) 4p–(^3P) 4d transition array, very good agreement was found with Djurović et al. (2013). In fact, the difference between our widths and those of Djurović et al. (2013) does not exceed 34 per cent except for one transition: $^2D^o_{3/2}$–$^2P_{3/2}$ ($\lambda = 3204.32$ Å), for which the ratio W_m/W is 1.42. Note that we have not taken into account the ion-impact Stark width for this line because the impact approximation is not valid. Our results agree with Pellerin et al. (1997) within 20 per cent on average. A very large disagreement with the results of Pellerin et al. (1997) was found for the transitions $^4D^o_{5/2}$–$^4D_{7/2}$ ($\lambda = 3844.73$ Å) and $^2D^o_{5/2}$–$^4D_{3/2}$ ($\lambda = 3958.38$ Å), for which the ratio W_m/W is 0.33 and 0.17, respectively. Note that for the $^4D^o_{5/2}$–$^4D_{7/2}$ transition, our Stark width agrees very well with Djurović et al. (2013) ($W_m/W = 0.96$) and that the width measured by Djurović et al. (2013) is larger than that of Pellerin et al. (1997) by a factor of 3. For the $^2D^o_{5/2}$–$^4D_{3/2}$ transition also, very good agreement is found with Djurović et al. (2013) ($W_m/W = 0.90$), whereas the ratio between the two experimental results is greater than 5. This large disagreement between the experimental results is explained in Djurović et al. (2013) by the self-absorption effect. Our Stark width agrees well with Aparicio et al. (1998) (about 15 per cent on average). There is only one exception, for the transition $^4D^o_{5/2}$–$^4F_{7/2}$ ($\lambda = 3576.62$ Å). In fact, for this transition, the ratio W_m/W varies from 1.89 to 1.98 in the temperature interval from 18 400 to 26 500 K. However, for the same transition, there is very good agreement with Pellerin et al. (1997) ($W_m/W = 1.02$) and with Djeniže et al. (1989) also ($W_m/W = 1.14$). Comparing with Djeniže et al. (1989), we find also good agreement (12 per cent on average). In Fig. 3, we show the temperature dependence of our electron-impact Stark width along with the experimental results for the (^3P) 4p $^4D^o_{7/2}$–(^3P) 4d $^4D_{7/2}$ ($\lambda = 3780.84$ Å) spectral line. Fig. 3 shows that our width is close to the experimental results of Pellerin et al. (1997), Djurović et al. (2013) and Djeniže et al. (1989). Fig. 3

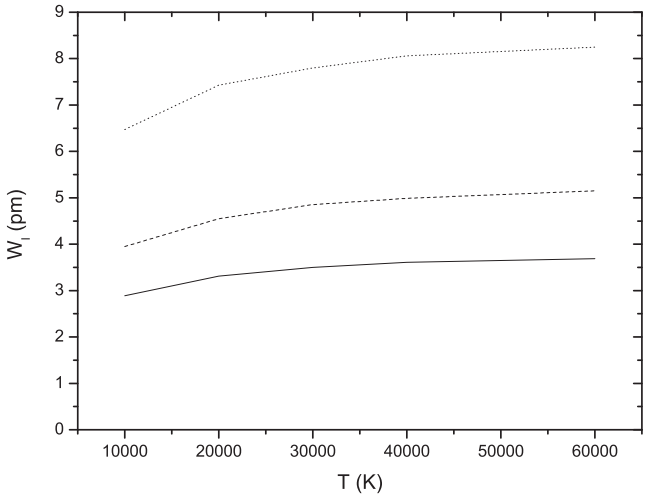

Figure 4. Temperature dependence of Ar II Stark widths due to collisions with positive ions (Ar^+) for an electron density of 10^{17} cm^{-3}. Solid line: (^{3}P) 3d ^{4}D$_{7/2}$–(^{3}P) 4p ^{4}D$^o_{7/2}$ ($\lambda = 4013.86$ Å) spectral line. Dashed line: (^{3}P) 4s ^{4}P$_{3/2}$–(^{3}P) 4p ^{4}P$^o_{1/2}$ ($\lambda = 4847.81$ Å) spectral line. Dotted line: (^{3}P) 4p ^{4}D$^o_{7/2}$–(^{3}P) 4d ^{4}D$_{7/2}$ ($\lambda = 3780.84$ Å) spectral line.

shows also that the result of Aparicio et al. (1998) is higher than our width by about 47 per cent.

For the (^{1}D) 4p–(^{1}D) 4d transition array, we do not give the Stark width (W_i) due to the impacts with positive ions because the impact approximation is not valid. The difference between our electron-impact Stark widths and the results of Aparicio et al. (1998) does not exceed 30 per cent. Our electron-impact Stark widths agree with the results of Djurović et al. (2013) within 31 per cent on average. Comparing with Pellerin et al. (1997), our results are in good agreement (better than 25 per cent) for four transitions. For three transitions, the difference is between 39 per cent and 61 per cent. For the transition ^{2}P$^o_{3/2}$–^{2}D$_{5/2}$ ($\lambda = 3639.83$ Å), we obtain a very large disagreement with Pellerin et al. (1997) ($W_m/W = 0.17$). On the other hand, our Stark width agrees very well with Djurović et al. (2013) ($W_m/W = 0.89$) for this transition. The large difference between the experimental results (factor of 5) is also explained in Djurović et al. (2013) by the self-absorption effect. Our results are compared with Djeniže et al. (1989) for three spectral lines. For two spectral lines, the agreement with Djeniže et al. (1989) is acceptable ($W_m/W = 0.74$) but for the transition (^{1}D) 4p ^{2}D$^o_{5/2}$–(^{1}D) 4d ^{2}D$_{5/2}$ ($\lambda = 3803.17$ Å), the value measured by Djeniže et al. (1989) is lower than our width by a factor of 3. The value in Djeniže et al. (1989) for this line is also very small compared with the results of Pellerin et al. (1997), Aparicio et al. (1998) and Djurović et al. (2013).

For the (^{3}P) 4p–(^{3}P) 5s, (^{3}P) 4p–(^{1}D) 5s, (^{1}D) 4p–(^{1}D) 5s and (^{1}S) 4s–(^{3}P) 5p transition arrays, our Stark widths agree well with all the experimental results and with the theoretical results of Griem (1974). In Fig. 4, we present the temperature dependence of Ar II Stark widths due to collisions with positive ions (Ar^+) for an electron density of 10^{17} cm^{-3} for three spectral lines: (^{3}P) 3d ^{4}D$_{7/2}$–(^{3}P) 4p ^{4}D$^o_{7/2}$ ($\lambda = 4013.86$ Å), (^{3}P) 4s ^{4}P$_{3/2}$–(^{3}P) 4p ^{4}P$^o_{1/2}$ ($\lambda = 4847.81$ Å) and (^{3}P) 4p ^{4}D$^o_{7/2}$–(^{3}P) 4d ^{4}D$_{7/2}$ ($\lambda = 3780.84$ Å). Unlike the electron-impact Stark width, Fig. 4 shows that the Stark width due to collisions with positive ions increases when the temperature increases. This is because the Coulomb repulsion decreases when the temperature increases.

Table 2. Our electron-impact Stark widths (W_e) compared with the results of Dimitrijević & Truong-Bach (1986) and Dimitrijević & Csillag (2006) (W_D). W_e is calculated with the SCP approach (Sahal-Bréchot 1969a,b) and a set of atomic data determined using the Cowan code (Cowan 1981). W_D is calculated with the SCP approach (Sahal-Bréchot 1969a,b), energy levels from Bashkin & Stoner (1975) and oscillator strengths calculated using the Bates & Damgaard method in Dimitrijević & Csillag (2006) and a scaled Thomas–Fermi model (Stewart & Rotenberg 1965) in Dimitrijević & Truong-Bach (1986). References: a Dimitrijević & Csillag (2006) and b Dimitrijević & Truong-Bach (1986).

Transition	T (K)	N_e (cm^{-3})	W_e (pm)	W_D (pm)	Reference
(^{3}P) 4s ^{2}P$_{1/2}$–(^{3}P) 4p ^{2}P$^o_{3/2}$	1000	10^{14}	0.178	0.193	a
$\lambda = 4764.86$ Å	2000	10^{14}	0.119	0.132	
	5000	10^{14}	0.0785	0.0859	
	10000	10^{14}	0.0583	0.0633	
	20000	10^{14}	0.0442	0.0474	
	50000	10^{14}	0.0352	0.0368	
(^{3}P) 4s ^{4}P$_{5/2}$–(^{3}P) 4p ^{4}P$^o_{5/2}$	1000	10^{14}	0.165	0.147	a
$\lambda = 4806.02$ Å	2000	10^{14}	0.107	0.110	
	5000	10^{14}	0.0705	0.0728	
	10000	10^{14}	0.0538	0.0544	
	20000	10^{14}	0.0410	0.0410	
	50000	10^{14}	0.0327	0.0317	
(^{3}P) 4s ^{2}P$_{3/2}$–(^{1}D) 4p ^{2}P$^o_{1/2}$	5000	10^{17}	48.1	37.5	b
$\lambda = 2891.61$ Å	10000	10^{17}	36.7	30.0	
	20000	10^{17}	28.8	24.3	
	30000	10^{17}	25.6	21.9	
	40000	10^{17}	23.8	20.7	
(^{3}P) 4s ^{2}P$_{3/2}$–(^{1}D) 4p ^{2}P$^o_{3/2}$	5000	10^{17}	46.6	38.8	b
$\lambda = 2942.89$ Å	10000	10^{17}	34.9	30.2	
	20000	10^{17}	26.8	24.0	
	30000	10^{17}	23.4	21.5	
	40000	10^{17}	21.7	20.3	
(^{3}P) 4s ^{2}P$_{1/2}$–(^{1}D) 4p ^{2}P$^o_{1/2}$	5000	10^{17}	51.0	39.7	b
$\lambda = 2979.05$ Å	10000	10^{17}	38.9	31.7	
	20000	10^{17}	30.5	25.8	
	30000	10^{17}	27.0	23.3	
	40000	10^{17}	25.2	22.1	
(^{3}P) 4s ^{2}P$_{1/2}$–(^{1}D) 4p ^{2}P$^o_{3/2}$	5000	10^{17}	49.4	41.1	b
$\lambda = 3033.51$ Å	10000	10^{17}	37.0	32.0	
	20000	10^{17}	28.4	25.5	
	30000	10^{17}	24.8	22.9	
	40000	10^{17}	22.9	21.6	
(^{3}P) 4p ^{2}P$^o_{3/2}$–(^{3}P) 4d ^{2}P$_{1/2}$	5000	10^{17}	99.4	118	b
$\lambda = 3366.58$ Å	10000	10^{17}	81.6	95.6	
	20000	10^{17}	71.7	79.9	
	30000	10^{17}	67.5	72.5	
	40000	10^{17}	64.9	67.9	
(^{3}P) 4p ^{2}P$^o_{1/2}$–(^{3}P) 4d ^{2}P$_{1/2}$	5000	10^{17}	95.6	114	b
$\lambda = 3307.23$ Å	10000	10^{17}	78.8	92.3	
	20000	10^{17}	69.3	77.1	
	30000	10^{17}	65.7	70.0	
	40000	10^{17}	63.4	65.6	
(^{3}P) 4p ^{2}P$^o_{3/2}$–(^{3}P) 4d ^{2}P$_{3/2}$	5000	10^{17}	104	148	b
$\lambda = 3293.64$ Å	10000	10^{17}	87.1	121	
	20000	10^{17}	76.3	99.9	
	30000	10^{17}	71.6	89.9	
	40000	10^{17}	68.5	83.4	
(^{3}P) 4p ^{2}P$^o_{1/2}$–(^{3}P) 4d ^{2}P$_{3/2}$	5000	10^{17}	100	143	b
$\lambda = 3236.81$ Å	10000	10^{17}	84.5	117	
	20000	10^{17}	74.1	96.6	
	30000	10^{17}	68.8	86.9	
	40000	10^{17}	65.9	80.7	
(^{3}P) 4p ^{2}D$^o_{3/2}$–(^{3}P) 4d ^{2}P$_{1/2}$	5000	10^{17}	98.7	107	b

Table 2 – *continued*

Transition	T (K)	N_e (cm^{-3})	W_e (pm)	W_D (pm)	Reference
$\lambda = 3273.32$ Å	10000	10^{17}	81.7	89.2	
	20000	10^{17}	71.8	75.6	
	30000	10^{17}	67.6	68.9	
	40000	10^{17}	65.1	64.6	
(^{3}P) 4p $^2D^o_{3/2}$–(^{3}P) 4d $^2D_{3/2}$	5000	10^{17}	102	74.9	b
$\lambda = 3000.44$ Å	10000	10^{17}	86.1	60.1	
	20000	10^{17}	74.6	51.3	
	30000	10^{17}	69.8	47.7	
	40000	10^{17}	66.7	45.5	
(^{3}P) 4p $^2D^o_{5/2}$–(^{3}P) 4d $^2D_{5/2}$	5000	10^{17}	103	66.0	b
$\lambda = 2955.39$ Å	10000	10^{17}	85.5	57.2	
	20000	10^{17}	73.3	50.5	
	30000	10^{17}	68.4	47.3	
	40000	10^{17}	65.2	45.4	
(^{3}P) 4p $^2D^o_{3/2}$–(^{3}P) 4d $^2D_{5/2}$	5000	10^{17}	108	69.5	b
$\lambda = 3014.48$ Å	10000	10^{17}	89.6	59.5	
	20000	10^{17}	76.5	52.5	
	30000	10^{17}	71.2	48.8	
	40000	10^{17}	67.9	46.7	

4 COMPARISON WITH PREVIOUS SEMICLASSICAL PERTURBATION CALCULATIONS

Dimitrijević & Truong-Bach (1986) calculated the Stark broadening parameters for 13 Ar II transitions belonging to the 4p–4d transition array. The calculations were carried out using the SCP approach, energy levels were taken from Bashkin & Stoner (1975) and oscillator strengths were calculated using a scaled Thomas–Fermi model (Stewart & Rotenberg 1965). To investigate the role of the Stark broadening mechanism on the mode structure of He–Ar gas lasers, Dimitrijević & Csillag (2006) calculated Stark broadening parameters for the (^{3}P) 4s ^{4}P–(^{3}P) 4p ^{4}P^o multiplet using a SCP approach. The energy levels were taken from Bashkin & Stoner (1975) and the oscillator strength was calculated using the Bates & Damgaard method.

In Table 2, we present our electron-impact Stark widths (W_e) compared with the results of Dimitrijević & Truong-Bach (1986) and Dimitrijević & Csillag (2006). The difference between our electron-impact Stark widths and the values of Dimitrijević & Csillag (2006) does not exceed 12 per cent. Compared with Dimitrijević & Truong-Bach (1986), the difference does not exceed 30 per cent, except for two transitions for which the difference is about 40 per cent.

5 LARGE-SCALE CALCULATIONS

Our large-scale calculations of Stark widths using the SCP approach (Sahal-Bréchot 1969a,b) and Cowan code (Cowan 1981) for atomic data are presented in Table 3. Only a sample of the results is provided to show the content of the additional data and their form. The complete results obtained for 300 spectral Ar II lines are given as additional data in electronic form in the online journal. The calculations have been made for a perturber density of 10^{17} cm^{-3} and for temperatures from 5000 to 60 000 K. Stark full widths at half intensity maximum (FWHM) are given for electron-, proton-, singly charged helium- and singly charged argon impact broadening. Since our results are obtained using calculated energy levels, a correction to the widths due to the difference between the calculated and observed wavelengths is introduced using equation (8) of Hamdi et al. (2013). All wavelengths given in Table 3 are taken from the National Institute of Standards and Technology (NIST).

In Table 3, we also specify a parameter C (Dimitrijević & Sahal-Bréchot 1984), which gives an estimate for the maximal perturber density for which the line may be treated as isolated when it is divided by the corresponding FWHM. For each value given in Table 3, the collision volume V multiplied by the perturber density N is much smaller than 1 and the impact approximation is valid (Sahal-Bréchot 1969a,b). For $NV > 0.5$, the impact approximation breaks down and thus, the values are not given. For $0.1 < NV \leq 0.5$,

Table 3. Electron, proton and singly-charged argon-impact Stark widths for Ar II lines calculated using the SCP approach (Sahal-Bréchot 1969a,b) and atomic data calculated using the Cowan code (Cowan 1981) for a perturber density of 10^{17} cm^{-3} and temperatures of 5000 to 60 000 K. The wavelength of the transitions (in Å) and parameter C (Dimitrijević & Sahal-Bréchot 1984) are also given. This parameter when divided with the corresponding Stark width gives an estimate for the maximal perturber density for which the line may be treated as isolated. W_e is the electron-impact full Stark width at half-maximum. W_{H^+} is the proton-impact full Stark width at half-maximum. W_{He^+} is the singly charged helium-impact full Stark width at half-maximum. W_{Ar^+} is the singly charged argon-impact full Stark width at half-maximum. For cells with an asterisk, the impact approximation reaches its limit of validity ($0.1 < NV \leq 0.5$). Empty cells mean that the impact approximation is not valid. This table is available in its entirety for 300 Ar II spectral lines in machine-readable form in the online journal as additional data. A portion is shown here to illustrate its form and content.

Transition	Temperature	W_e (Å)	W_{H^+} (Å)	W_{He^+} (Å)	W_{Ar^+} (Å)
(^{1}D) 4s $^2D_{5/2}$–(^{1}D) 4p $^2F^o_{7/2}$	5000	0.761	0.375E-01	0.461E-01	0.556E-01*
4609.57 Å	10000	0.575	0.545E-01	0.612E-01	0.666E-01*
$C = 0.13E+21$	20000	0.441	0.652E-01	0.700E-01	0.758E-01*
	30000	0.388	0.703E-01	0.748E-01	0.790E-01*
	40000	0.359	0.738E-01	0.778E-01	0.805E-01*
	60000	0.327	0.785E-01	0.803E-01	0.822E-01
(^{3}P) 4p $^4P^o_{1/2}$–(^{3}P) 4d $^4P_{3/2}$	5000	0.701	0.381E-01	0.438E-01*	–
3249.80 Å	10000.	0.541	0.557E-01	0.555E-01*	–
$C = 0.21E+20$	20000.	0.446	0.676E-01	0.659E-01*	0.647E-01*
	30000	0.419	0.743E-01	0.707E-01	0.671E-01*
	40000	0.404	0.803E-01	0.750E-01	0.690E-01*
	60000	0.387	0.866E-01	0.792E-01	0.719E-01*

the impact approximation reaches the limit of validity and values are marked with an asterisk.

All the Stark widths presented in Table 3 will be inserted into the STARK-B data base (Sahal-Bréchot et al. 2015, http://stark-b.obspm.fr/), which contains widths and shifts of isolated lines of neutral and ionized elements due to electron and ion impact. It is devoted to modelling and spectroscopic diagnostics of stellar atmospheres and envelopes, laboratory and fusion plasmas, laser equipment and technological plasmas. STARK-B is a node of the Virtual Atomic and Molecular Data Center (Dubernet et al. 2016, http://www.vamdc.org/).

6 CONCLUSIONS

Using atomic data from the Cowan code (Cowan 1981) and the impact SCP approach, we have calculated Stark widths for 300 spectral lines of singly charged argon. The comparison of our widths with experimental and theoretical values in the literature shows that our results are generally in good agreement for most spectral lines. The best agreement was with Djurović et al. (2013) and the worst agreement was with Dzierzega & Musiol (1994). For a number of spectral lines, our results agree with some authors and not with others. The comparison between experimental and theoretical results suggests that both theories and experiments can be improved. Our Stark widths may be of interest for modelling and investigations of A-type and B-type stars and also subdwarfs, since Ar II spectral lines are observed in these kinds of stars. Our results may also be of interest for laser physics and diagnostics of laboratory plasmas.

ACKNOWLEDGEMENTS

This work is part of project 'Influence of collisional processes on astrophysical plasma line shapes' (176002) supported by the Ministry of Education, Science and Technological Development of Serbia. This work has also been supported by the Paris Observatory, the CNRS and Programme National de Physique Stellaire, INSU-CNRS, France.

REFERENCES

Aparicio J. A., Gigosos M. A., González V. R., Pérez C., de la Rosa M. I., Mar S., 1998, J. Phys. B, 31, 1029
Bashkin S., Stoner J. O., 1975, Atomic Energy Levels and Grotrian Diagrams, Vol. II. North Holland and Elsevier, Amsterdam
Blanchette J.-P., Chayer P., Wesemael F., Fontaine G., Fontaine M., Dupuis J., Kruk J. W., Green E. M., 2008, ApJ, 678, 1329
Cowan R. D., 1981, The Theory of Atomic Structure and Spectra, University of California Press, Berkeley, USA
Dimitrijević M. S., Csillag L., 2006, J. Applied Spectrosc., 73, 458
Dimitrijević M. S., Konjević N., 1980, J. Quant. Spectrosc. Radiat. Transfer, 24, 451
Dimitrijević M. S., Sahal-Bréchot S., 1984, J. Quant. Spectrosc. Radiat. Transfer, 31, 301
Dimitrijević M. S., Sahal-Bréchot S., 1996, Phys. Scr., 54, 50
Dimitrijević M. S., Truong-Bach, 1986, Z. Naturforsch A, 411, 772
Dimitrijević M. S., Sahal-Bréchot S., Bommier V., 1991, A&AS, 89, 581
Dimitrijević M. S., Simić Z., Kovačević A., Valjarević A., Sahal-Bréchot S., 2015, MNRAS, 454, 1736
Djeniže S., Malešević M., Srécković A., Milosavljević M., Purić J., 1989, J. Quant. Spectrosc. Radiat. Transf., 42, 429
Djurović S., Belmonte M. T., Peláez R. J., Aparicio J. A., Mar S., 2013, MNRAS, 433, 1082
Dubernet M. L. et al., 2016, J. Phys. B, 49, 074003
Dzierzega K., Musiol K., 1994, J. Quant. Spectrosc. Radiat. Transf., 52, 747
Fleurier C., Sahal-Bréchot S., Chapelle J., 1977, J. Quant. Spectrosc. Radiat. Transfer, 17, 595
Gajo T., Mijatović Z., Savić I., Djurović S., Kobilarov R., 2013, J. Quant. Spectrosc. Radiat. Transf., 127, 119
Griem H. R., 1974, Spectral Line Broadening by Plasmas, Academic Press, Inc., New York
Hamdi R., Ben Nessib N., Milovanović N., Popović L. Č., Dimitrijević M. S., Sahal-Bréchot S., 2008, MNRAS, 387, 871
Hamdi R., Ben Nessib N., Dimitrijević M. S., Sahal-Bréchot S., 2011, Baltic Astron., 20, 552
Hamdi R., Ben Nessib N., Dimitrijević M. S., Sahal-Bréchot S., 2013, MNRAS, 431, 1039
Hamdi R., Ben Nessib N., Sahal-Bréchot S., Dimitrijević M. S., 2014, Advances Space Res., 54, 1223
Hamdi R., Ben Nessib N., Sahal-Bréchot S., Dimitrijević M. S., 2017, Atoms, 5, 26
Heber U., Edelmann H., 2004, Ap&SS, 291, 341
Iglesias E. J., Ghosh J., Elton R. C., Griem H. R., 2006, J. Quant. Spectrosc. Radiat. Transf., 98, 101
Jeffery C. S., Woolf V. M., Pollacco D. L., 2001, A&A, 376, 497
Konjević N., Lesage A., Fuhr J. R., Wiese W. L., 2002, J. Phys. Chem. Ref. Data, 31, 819
Kramida A., Ralchenko Yu., Reader J., NIST ASD Team 2015, NIST Atomic Spectra Database (ver. 5.3). http://physics.nist.gov/asd. National Institute of Standards and Technology, Gaithersburg, MD
Lanz T., Cunha K., Holtzman J., Hubeny I., 2008, ApJ, 678, 1342
Naslim N., Geier S., Jeffery C. S., Behara N. T., Woolf V. M., Classen L., 2012, MNRAS, 423, 3031
Pellerin S., Musiol K., Chapelle J., 1997, J. Quant. Spectrosc. Radiat. Transf., 57, 377
Popović L. Č., Simić S., Milovanović N., Dimitrijević M. S., 2001, ApJS, 135, 109
Qian M., Ren C., Wang D., Zhang J., Wei G., 2010, J. Applied Phys., 107, 063303
Sahal-Bréchot S., 1969a, A&A, 1, 91
Sahal-Bréchot S., 1969b, A&A, 2, 322
Sahal-Bréchot S., 1974, A&A, 35, 319
Sahal-Bréchot S., 1991, A&A, 245, 322
Sahal-Bréchot S., Dimitrijević M. S., Ben Nessib N., 2014, Atoms, 2, 225
Sahal-Bréchot S., Dimitrijević M. S., Moreau N., Ben Nessib N., 2015, Phys. Scr., 90, 054008
Simić Z., Dimitrijević M. S., Milovanović N., Sahal-Bréchot S., 2005, A&A, 441, 391
Simić Z., Dimitrijević M. S., Kovačević A., 2009, New Astron. Rev., 53, 246
Stewart J. C., Rotenberg M., 1965, Phys. Rev., 140, 1508
Wesemael F., 1981, ApJS, 45, 177

SUPPORTING INFORMATION

Supplementary data are available at *MNRAS* online.

Table 3. Electron, proton and singly-charged argon-impact Stark widths for Ar II lines calculated using the SCP approach (Sahal-Bréchot 1969a,b) and atomic data calculated using the Cowan code (Cowan 1981) for a perturber density of 10^{17} cm^{-3} and temperatures of 5000 to 60 000 K.

Please note: Oxford University Press is not responsible for the content or functionality of any supporting materials supplied by the authors. Any queries (other than missing material) should be directed to the corresponding author for the article.

This paper has been typeset from a TEX/LATEX file prepared by the author.